Advanced Composite Materials
Publication details, including instructions for authors and subscription information:
http://www.tandfonline.com/loi/tacm20

Effect of nanoclay in HDPE-glass fiber composites on processing, structure, and properties

Mohan T.P. & K. Kanny [a]
[a] Composites Research Group, Department of Mechanical Engineering, Durban University of Technology, Durban, South Africa
Version of record first published: 23 Oct 2012.

To cite this article: Mohan T.P. & K. Kanny (2012): Effect of nanoclay in HDPE-glass fiber composites on processing, structure, and properties, Advanced Composite Materials, 21:4, 315-331

To link to this article: http://dx.doi.org/10.1080/09243046.2012.736348

Advanced Composite Materials
Vol. 21, No. 4, August 2012, 315–331

Effect of nanoclay in HDPE–glass fiber composites on processing, structure, and properties

Mohan T.P. and K. Kanny*

Composites Research Group, Department of Mechanical Engineering, Durban University of Technology, Durban, South Africa

(*Received 15 February 2011; accepted 16 July 2012*)

Natural Na^+ montmorillonite (MMT) microclay and organo-treated MMT nanoclay were independently filled in a high-density polyethylene (HDPE) polymer and HDPE–glass fiber (GF) composite and the rheological and mechanical properties were examined. The addition of nanoclay in the HDPE polymer and HDPE–GF composite increased the melt viscosity, rate of crystallization, and crystalline fraction. Addition of Na^+ MMT clay on the other hand did not affect the crystalline properties, but increased the melt viscosity marginally. The composite was also examined after the addition of a polyethylene-grafted maleic anhydride-based compatibilizer. It was found that the compatibilizer improved the dispersion of clay particles in the polymer matrix which in turn affected the rheological and mechanical properties of the composite. Improved tensile and wear properties were observed in nanoclay-filled composites when compared to microclay-filled composites.

Keywords: nanoclay; glass fiber-reinforced plastics; high-density polyethylene; polymer–clay nanocomposites

1. Introduction

Fiber-reinforced high-density polyethylene (HDPE)-based thermoplastic composites are used in various engineering application due to their light weight, easy processing, enhanced rigidity, and strength. HDPE-based composites are frequently used in the manufacture of cables, impellers, and liners as well as in other engineering products. Fairly often, this composite material fails during usage due to their poor matrix-related properties or fiber–matrix interface properties [1–3]. Attempts to improve the properties of composites by a blending method in which a second phase polymer is added to assist the processing have been made [4,5]. Few studies are focused towards enhancing property of composites by selecting and positioning high strength fiber and tuning volume fraction [6–9]. Reports on improving the interface properties of matrix and fiber through coupling and compatibilizer method are available [10–12]. Very few studies on the failure problem have been found in the literature. Therefore, the aim of this present work is to solve this failure problem in HDPE–glass fiber (GF) composites using nanoclay as the reinforcement. The purpose of selecting nanoclay as the reinforcement is because of improved property at lower concentration and also easy to process this three-phase system (matrix–clay–GF).

*Corresponding author. Email: kannyk@dut.ac.za

ISSN 0924-3046 print/ISSN 1568-5519 online

http://dx.doi.org/10.1080/09243046.2012.736348
http://www.tandfonline.com

Clay fillers used in polymer matrix are usually montmorillonite (MMT)-based clay. Each MMT clay particle consists of several nano disks (sheet) like structure with thickness of 1 nm and length of several 100 nm. Each sheet is made up of alumina–silica tetraheadral/octahedral crystal structure and arranged parallel to each other. The distance between each layer is called as interlayer spacing or *d*-spacing. In the interlayer spacing exchangeable Na^+ ions are present and make this clay a hydrophilic in nature [13–15]. Organic polymers on the other hand are hydrophobic in nature and therefore MMT clays do not show miscible mixture to the organic polymer. To render clay compatible to organic polymer, an organic treatment is usually given to MMT clay. In organic treatment of clays, the Na^+ cations are replaced by quarternary or onium ions into intergallery regions of clay nanolayer spacing. These ions attract the hydrophobic matrix polymer and aids in the dispersion of nanolayers in polymer matrix, thereby forms a nanolayer dispersed polymer nanocomposites. In this present work, natural Na^+ MMT is referred to as microclay and organo-treated MMT clay is referred to as a nanoclay.

At very low nanoclay concentrations (about 3 wt.%) in polymer matrix, superior improvement in properties (physical, thermal, and mechanical) is observed. If MMT clays are untreated and added into the matrix polymer very little improvement in property is observed, since the clay acts only as a micron-scale filler particle in polymer matrix. The addition of organo-treated nanoclay in polymer matrix leads to the two different types of nanocomposite structure, namely, an intercalated and an exfoliated nanocomposite structure. In the intercalated nanocomposite structure, the polymer matrix entered into the interlayer spacing of the nanoclay and increases the nanolayers spacing, but still maintains the regular arrangement of nanolayers in the polymer matrix. In the exfoliated nanocomposite structure, the polymer matrix enters into the interlayer spacing of the nanoclays and makes the nanolayers to separate (or delaminate) further and disperse them randomly in the polymer matrix. Exfoliated nanocomposite shows improved properties than that of intercalated nanocomposite structure [16–18]. Achieving an exfoliated structure is an important objective in the polymer–clay nanocomposites. Moreover, in nonpolar polymer such as HDPE, it is necessary to add compatibilizer to have good compatibility between the matrix and the nanoclay and also to have good exfoliated structure. The compatibilzier consists of nonpolar and polar group and thereby serve as a bridge between the nonpolar matrix polymer and the polar nanoclays. Several types of compatibilizers are available in literature showing exfoliated nanocomposite structure and among them polyethyelene-grafted maleic anhydride (gMA) compatibilizer provides good compatibility for olefins-based nanoclay composites [17, 19–22].

This study is on the development of hybrid HDPE composites consisting of a three-phase material system, namely, matrix (polymer), clay filler (as secondary reinforcement), and GF (as a primary reinforcement). The study is important because very little data are available for this type of hybrid composite material [23–25]. In these works, the matrix and the reinforcement material are either thermoset epoxy or wood flour particles and their manufacturing and processing behaviors are entirely different. As discussed earlier, HDPE composites are used in several engineering applications and frequent failures occur due to their weak fiber matrix interphase and matrix property. Hence, it is important to examine the effect of clay addition on the property of HDPE composites. Specific attention on the tensile property and wear behaviors of HDPE–fiber composites is studied. To study this effect, nanoclay and microclay of 3 wt.% are filled individually in GF-reinforced HDPE composites. The GF of 20% volume is considered in the present work. The effect of compatibilizer on the hybrid composites (clay–HDPE–GF) is also studied.

2. Experimental details

2.1. Raw material

A HDPE polymer of melting point 138 °C and chopped-GF of length of 25 ± 5 mm (Aspect ratio of 150) were procured from AMT Composites, Durban-South Africa. Polyethylene gMA was procured from Arkema Group, USA supplied under the trade name of Orevac-18510P. Quaternary ammonium salt modified montmorillonite nanoclay (Cloisite 15A) and unmodified clay (Na^+ Cloisite) were procured from Southern Clay Products Inc, USA.

2.2. Composites processing

The HDPE hybrid composite was manufactured using a melt-blending technique. Here, the HDPE pellets, GF, clay, and gMA, were mixed together in a Reiffenhaeuser single-screw extruder. The extruder has a 40 mm diameter single rotating screw with a length/diameter ratio of 24 and driven by a 7.5 kW motor. It has three heating zones along the length of the screw as follows: Zone 1 (Hopper or pellet loading end), Zone 2 (center region of screw), and Zone 3 (extrusion end). The melt mixing processing conditions were kept at 130 °C (Zone 1), 170 °C (Zone 2), and 170 °C (Zone 3) with the extrusion screw speed set at 100 rpm. Table 1 shows the list of materials processed for this study. In all these material development, the processing condition was kept the same as per above discussion. The molten samples coming from extrusion nozzle were rapidly quenched to room temperature using water.

2.3. Characterization

Melt flow index was measured for test samples using ASTM D1238 standard. Thermal analyzer differential scanning calorimetry (DSC) instrument was used to heat the sample from room temperature to 180 °C at the heating rate of 10 °C/min. The crystallization and melting peak details were observed from DSC result. Crystalline fraction in the composite system was calculated by measuring the ratio of ΔH (J/g) value of melting peak of test specimen to that of theoretically 100% crystalline HDPE polymer (292 J/g) [26]. Crystallization rate was measured in composites series by placing the samples at their respective crystallization temperature for different time periods and then rapidly quenching in cold water at the rate of 100 °C/min. The quenched specimen was further heat scanned using DSC to measure the crystalline properties.

The structure of nanocomposites was studied using X-ray diffraction (XRD) and transmission electron microscopy (TEM) analysis. A Philips PW1050 diffractometer was used to

Table 1. List of materials processed for study.

S. No	Material
1	HDPE
2	HDPE + 3% nanoclay
3	HDPE + 3% nanoclay + 3% gMA
4	HDPE + 3% microclay
5	HDPE + 3% microclay + 3% gMA
6	HDPE + 20% (volume) GF
7	HDPE + 20% GF + 3% nanoclay
8	HDPE + 20% GF + 3% nanoclay + 3% gMA
9	HDPE + 20% GF + 3% microclay
10	HDPE + 20% GF + 3% microclay + 3% gMA

obtain the X-ray diffraction patterns using CuKα lines ($\lambda = 1.5406$ Å). The diffractograms were scanned from 2.5° to 30° (2θ) in steps of 0.02° using a scanning rate of 0.5°/min. Microscopic investigation of selected nanocomposite specimens at the various weight compositions were conducted using a Zeiss scanning transmission electron microscope with an operating voltage of 20–120 kV. Tensile tests were performed on specimens using the LLOYDS Tensile Tester fitted with a 20 kN load cell. The tests were performed at a crosshead speed of 1 mm/min in accordance with the ASTM D3039 standard. Five tensile specimens were taken and the average value was considered for plotting stress–strain curves and maintaining the standard deviation of all the test specimens within 3%. Tensile-fractured samples were analyzed using JEOL JSM 840A scanning electron microscope (SEM). Further, pin-on-disk wear test of the specimens was carried out. Test was carried out using locally manufactured tribometer in accordance with ASTM G-99 standard. It consists of a loading disk, where loads are kept and applied over square pins. The dimension of the wear test pins is 8 mm^2 and 20 mm in length. The disk used was brass of surface roughness 0.2 m. A constant contact pressure of 0.15 MPa and sliding velocity of 0.35 m/s is applied and percentage weight loss of the test pin for the sliding distance of 3600 m is measured. Wear tracks of pins were observed using ZEISS AXIO LAB optical microscope.

3. Results and discussions

3.1. Rheology

Table 2 shows the melt flow rate of unfilled and clay-filled HDPE and HDPE–GF composite series. The addition of clay (nanoclay and microclay) and gMA in HDPE and HDPE–GF composites reduces the melt flow rate. Nanoclay-filled composites show enhanced viscosity than unfilled and microclay-filled composites.

Figures 1 and 2 show the DSC heating scans of nanoclay- and microclay-filled composite series, respectively, and the corresponding DSC results (T_{ch}, T_{cc}, and crystalline fraction) are shown in Table 3. The DSC parameters, namely, T_{ch} and T_{cc} are the crystallization temperature of the sample during heating and cooling, respectively. Crystalline fraction is the measure of the amount of crystallinity part of the total system. Results indicate that the nanoclay addition in HDPE polymer increases T_{ch}, T_{cc}, and crystalline fraction. However, microclay addition does not show improvement in T_{ch}, T_{cc}, and crystalline fraction values of base HDPE polymer. The gMA addition in HDPE–clay composites retards the T_{ch}, T_{cc}, and crystalline fraction; however, the values are higher than that of unfilled polymer and polymer–GF composites.

Table 4 shows the rate of crystallization of HDPE–clay–GF series. The rate of crystallization in nanoclay-filled HDPE composites was higher than that of unfilled and microclay-filled

Table 2. Melt flow characteristics of HDPE–clay series.

	Melt flow rate (g/min)	
Material	Nanoclay series	Microclay series
HDPE	10	10
HDPE + 3% clay	8	9
HDPE + 3% clay + 3% gMA	6	7
HDPE + GF	6	6
HDPE + GF + 3% clay	4	5
HDPE + GF + 3% clay + 3% gMA	3	5

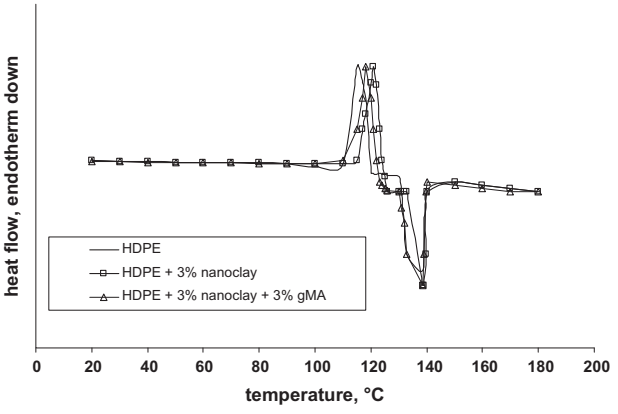

Figure 1. DSC heat-2 scan of HDPE–nanoclay series.

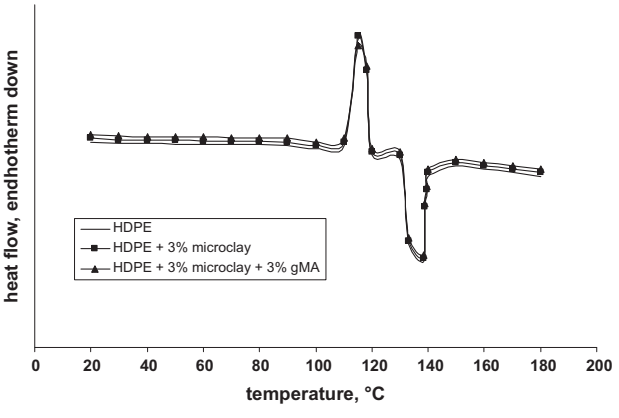

Figure 2. DSC heat-2 scan of HDPE–microclay series.

Table 3. DSC result of HDPE–clay series.

	T_{ch}		T_{cc}		Crystalline fraction	
Material	Nanoclay series	Microclay series	Nanoclay series	Microclay series	Nanoclay series	Microclay series
HDPE	115	115	118	118	62.0	62.0
HDPE + 3% clay	121	115	121	118	71.0	63.0
HDPE + 3% clay + 3% gMA	118	115	120	117	66.0	62.0
HDPE + GF	115	115	118	118	51.2	51.2
HDPE + GF + 3% clay	121	115	120	118	56.7	51.6
HDPE + GF + 3% clay + 3% gMA	119	115	119	118	53.3	50.7

composites. Addition of gMA in HDPE–nanoclay composites retards the rate of crystallization; however, the rate of crystallization is higher than that of HDPE polymer. Similar crystallization effect of gMA in ternary blends is reported elsewhere [27,28]. The increased crystalline

Table 4. Rate of crystalline formation of HDPE–GF–clay series.

	Crystalline fraction of composites series					
	Nanoclay series			Microclay series		
Material	1 min	2 min	3 min	1 min	2 min	3 min
HDPE	14	33	62	14	33	62
HDPE + 3% clay	18	41	71	16	31	63
HDPE + 3% clay + 3% gMA	16	37	66	17	30	62
HDPE + GF	17.3	34	51.2	17.3	34	51.2
HDPE + GF + 3% clay	21.7	37	54.1	17	35.1	51.6
HDPE + GF + 3% clay + 3% gMA	20.1	34.3	52.3	17.3	34.7	50.7

fraction and rate of crystallization in nanoclay-filled composites may be attributed to the nano-level dispersion of clay in the polymer matrix. This nano dispersion of clays in polymer possibly acts as a nucleation site during synthesis and may have improved the crystalline properties.

To understand this crystallization behavior the Avarami equation was used. Equation (1) shows the Avarami equation as a function of relative crystallinity (X_r) and time (t) to achieve X_r:

$$X_r(t) = 1 - \exp(-Kt^n) \tag{1}$$

The K and n are constants that are considered as the important parameters for crystallization mechanisms.

The values of K and n can be calculated by plotting $\log[-\ln(1-X_r)]$ vs. $\log(t)$. n and $\log(K)$ values are the slope and intercept values, respectively, of the Avarami's plot. The Avarami plot for HDPE–clay series and HDPE–GF–clay series is shown in Figures 3 and 4, and their respective n and K values are shown in Table 5. The result shows improved K with reduced n values in nanoclay-filled composites. This increased kinetic constant (K), crystallization rate, and decreased n value of nanoclay-filled composites suggest that the nanoclay acts as the nucleating agent in the system, thereby increasing the crystalline fraction and the rate of crystallization [20–22]. The unfavorable kinetic constants (K and n) in unfilled and microclay- and gMA-filled composites, however, suggest lower nucleation effect in the system.

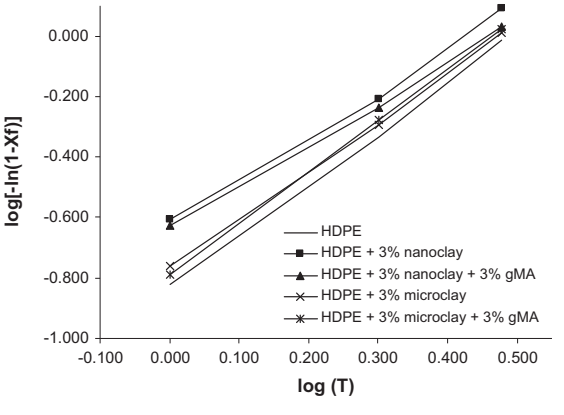

Figure 3. Avarami plot of HDPE–clay series.

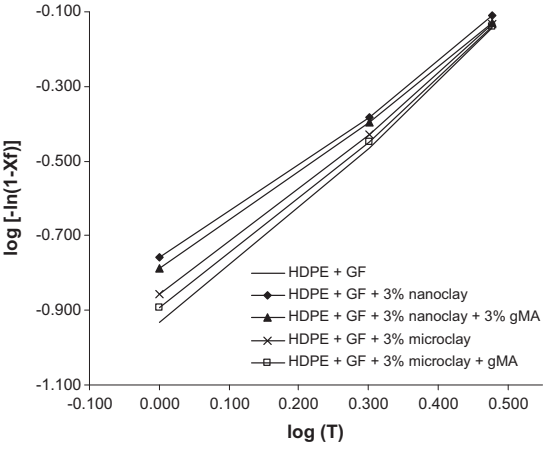

Figure 4. Avarami plot of HDPE–GF–clay series.

Table 5. Avarami's constant of composites series.

	Nanoclay series		Microclay series	
Material	n	K (min^{-n})	n	K (min^{-n})
HDPE	1.683	0.082	1.683	0.082
HDPE + 3% clay	1.375	0.199	1.603	0.118
HDPE + 3% clay + 3% gMA	1.445	0.211	1.603	0.118
HDPE + GF	1.643	0.027	1.643	0.027
HDPE + 3% clay + GF	1.350	0.116	1.570	0.046
HDPE/GF + 3% clay + 3% gMA	1.370	0.102	1.502	0.066

3.2. Structure of nanocomposites

Figure 5 shows the XRD patterns of the clay and the composite series. Cloisite-15A shows the diffraction peak at 2θ value of 3.3° and corresponds to the interlayer spacing of 26.75 Å (calculated as per Bragg's diffraction equation $2d\ Sin\theta = n\lambda$, where d is the interlayer spacing

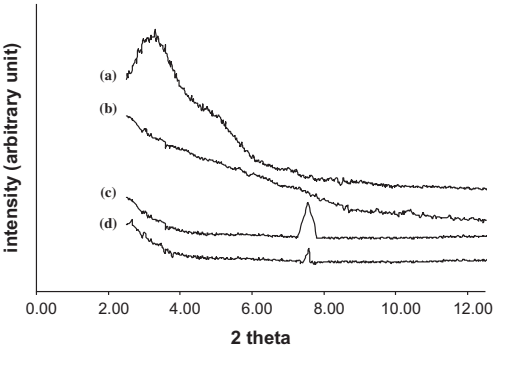

Figure 5. XRD pattern of (a) nanoclay, (b) HDPE–nanoclay–gMA, (c) microclay, and (d) HDPE–microclay–gMA.

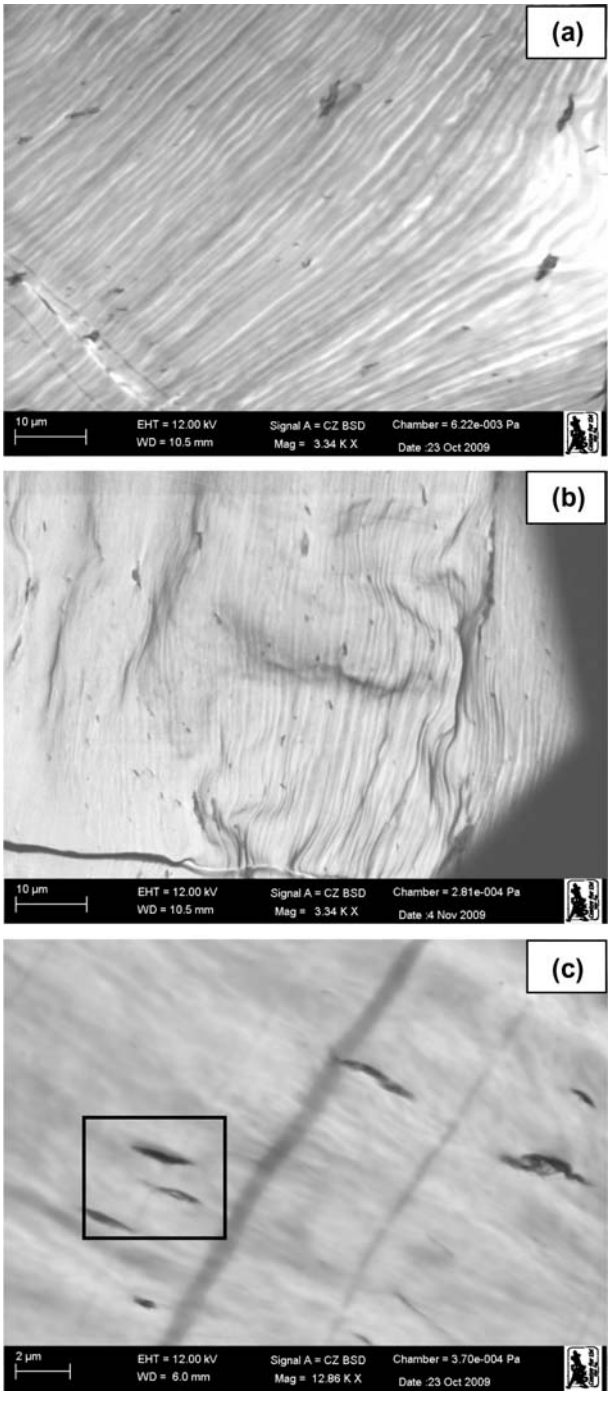

Figure 6. TEM of 3% nanoclay-filled HDPE (a) without gMA, (b) with gMA, and (c) high magnification TEM of HDPE–nanoclay–gMA.

of nanoclay; θ = reflection angle; n = order of reflection and it is 1; and λ = wavelength of X-ray used for diffraction experiment). The XRD pattern of 3 wt.% nanoclay-filled HDPE composites does not show any diffraction peak of nanoclay. This result suggests that the matrix HDPE polymer has entered into the clay's interlayer spacing and may have caused the random (or delaminated) dispersion of clay nanolayers in the polymer matrix. This type of random (or delaminated) arrangement of clay nanolayers in polymer matrix is called as an exfoliated structure [13–15]. Na^+ Cloisite (microclay) shows the diffraction peak at 2θ of 7.58° and corresponds to the interlayer spacing of 11.68 Å. Moreover, the XRD pattern of 3 wt.% microclay-filled HDPE composites also show the diffraction peak at 2θ of 7.58° value and this corresponds to the interlayer spacing of Na^+ Cloisite (microclay) of 11.68 Å. This result suggests that the matrix HDPE polymer has not entered into the microclay's interlayer spacing and therefore no nanolayer dispersions has occurred. This suggests that Na^+ Cloisite clays are dispersed in the HDPE matrix as micron-scale filler due to the absence of nanolayer dispersions in matrix.

To further understand the structure of composites, TEM pictures of composite series were taken and examined. Figure 6 shows the bright field TEM pictures of 3 wt.% nanoclay-filled HDPE composites with and without gMA. The bright region is the matrix phase and the dark phase is the nanoclay phase. In HDPE– 3 wt.% nanoclay composites, the TEM picture (Figure 6(a)) shows some agglomeration of clay particles in matrix, whereas the TEM picture of (Figure 6(b)) gMA-filled nanocomposites shows better dispersion of particles in the matrix. The gMA acts as a compatibilizer between clay and matrix phase and aids better dispersion of particles in matrix polymer. It should be noted that the nanoclay and HDPE polymer are an immiscible blend. HDPE is a nonpolar polymer phase, whereas alkyl ammonium organo ion of nanoclay is a polar phase, thereby resulting in immiscible blends. This immiscibility of blends causes improper dispersion of clay in polymer matrix, whereas PE-gMA compatibilizer addition in HDPE–clay mixture causes the miscible blends. In the PE-gMA, the polyethylene forms miscible blend with HDPE polymer and MA (maleic anhydride) reacts with the organo ions of nanoclay and the resultant structure forms a miscible blend. This miscible blend improves the dispersion of the clay phase in the polymer matrix as reported elsewhere [17,20,29]. Figure 6(c) shows high magnification of TEM of HDPE–clay–gMA composites and shows the formation of an exfoliated nanocomposite structure. The nanoclay layers are well separated and forms an exfoliated nanocomposite. This result is supported by the XRD data. To confirm the existence of clay phase in the TEM image an energy dispersive X-ray (EDX) test was performed on the selective area of the TEM image (the chosen area is represented in the square bracket) to verify the presence of clay phase. Figure 7 shows the EDX pattern of the specimen and the values are

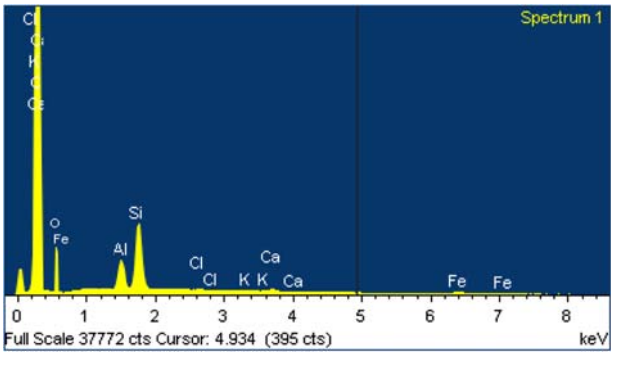

Figure 7. EDX image of HDPE–3% nanoclay–gMA composites.

Table 6. Elemental analysis of HDPE–3% nanoclay–gMA composites.

Element	Weight (%)
C	96.31
O	1.39
Al	0.31
Si	0.63
Other trace elements	1.36

shown in Table 6. The result shows the carbon as a major element (due to HDPE) with a lower amount of O, Al, and Si, which is possibly due to the presence of clay in the composite. A standard mineral data of elements of MMT clays show about 10% Al and 21% Si, and in oxide form MMT has about 19% Al_2O_3 and 44% SiO_2 phases [30]. EDX result (Table 6) shows about 3% of Al and Si elements in the composites and hence correlates well with the experimental result and also confirms the presence of the clay phase in the TEM pictures.

Figure 8 shows the TEM of 3 wt.% microclay-filled HDPE composites with and without gMA. This TEM picture shows that the microclays (Na^+ Cloisite) dispersed in polymer

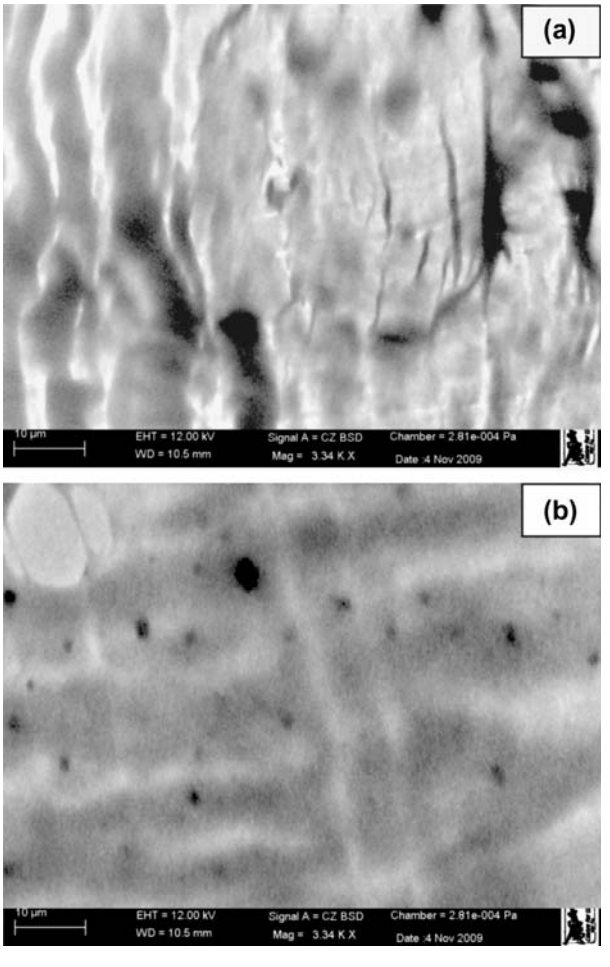

Figure 8. TEM of 3% microclay-filled HDPE (a) without gMA and (b) with gMA.

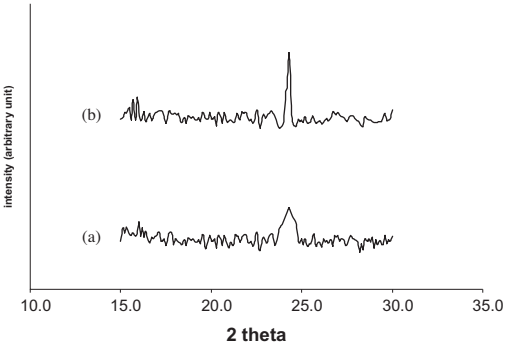

Figure 9. XRD patterns of (a) HDPE and (b) HDPE + 3 wt.% nanoclay.

matrix at micron level. Moreover, gMA filled Na^+ Cloisite (microclay) composites provide better dispersion of microclays in polymer matrix. Overall, the TEM results show better distribution of clays in gMA-filled composites. It may be concluded that the addition of compatilbilizers in HDPE–clay system improves the dispersions of particles, however, they affects the rheological characteristics (melt flow and crystallization) of composites. Figure 9 shows the XRD pattern of HDPE and HDPE + 3% nanoclay composites. Pure HDPE shows the broad XRD peak at 2θ value of 24.3°, whereas 3% nanoclay-filled HDPE composites show sharp peak with increased peak intensity value. This result suggests that 3% nanoclay-filled composites show increased crystalline fraction and thus correlates well with the DSC results.

3.3. *Tensile properties of HDPE–GF–clay composites*

The tensile stress–strain curve of HDPE–GF–clay composite series is shown in Figure 10. The tensile property of nanoclay- and gMA-filled HDPE–GF composite is better than that of

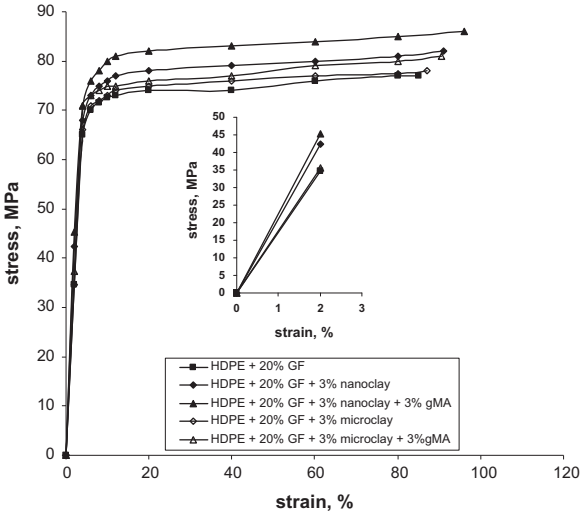

Figure 10. Tensile stress–strain curves of HDPE–GF-clay series.

Table 7. Tensile properties of HDPE–GF–clay composite series.

Material	Tensile strength (MPa)		Tensile modulus (GPa)		Strain at break (%)	
	Nanoclay series	Microclay series	Nanoclay series	Microclay series	Nanoclay series	Microclay series
HDPE-GF	77	77	17.3	17.3	85	85
HDPE-GF + 3% clay	82	78	21.2	17.7	91	87
HDPE-GF + 3% clay + 3% gMA	86	80	23.1	18.7	96	90

Table 8. Wear loss of HDPE–clay and HDPE–GF–clay series.

	Weight loss (%)	
Material	Nanoclay series	Microclay series
HDPE	6.4	6.4
HDPE + 3% clay	2.9	5.1
HDPE + 3% clay + 3% gMA	2.7	4.9
HDPE + GF	5.1	5.1
HDPE + GF + 3% clay	2.1	4.6
HDPE + GF + 3% clay + 3% gMA	1.9	4.2

microclay-filled and -unfilled composite series. Table 7 shows the tensile properties of composite series.

A 22.5% improvement in modulus is observed for nanoclay filled composites when compared to unfilled composites. Figure 10 shows the tensile stress–strain curves for the composite series up to failure load. It may be difficult to understand the changes taking place within the elastic limit and 0.2% offset stress–stress curves. Therefore, the elastic stress–strain curves of the selective composite series were enlarged and represented as an inserted tensile stress–strain curve in Figure 10. The inserted figure shows the level of improvement of modulus of the nanoclay-filled composites. Almost no improvement in tensile modulus was seen when the microclay is filled in HDPE–GF system; however, a small improvement was observed when gMA was added. The improvement of tensile modulus of nanoclay-filled composites series suggests that the nanoclay disperse in polymer matrix at molecular level and resists the molecular deformation under loading. Good improvements in tensile strain and strength values were observed when nanoclay was added to HDPE–GF composites. Microclay-filled composites did not show good improvement. Some enhancements in strain and strength values were observed in gMA-filled HDPE–microclay composites. The better dispersion of particles in gMA-filled HDPE–microclay composites may have caused the improved tensile property.

Figure 11 shows the SEM of tensile fracture surface of composites. In HDPE–GF fracture surface, some fiber pull-out was observed. The matrix fracture surface shows brittle and smooth fracture features. In HDPE–GF–nanoclay composites, the fracture surface of matrix shows crack fronts were branched and induced roughness at fracture surface. This branched propagation of crack in the matrix may have caused increased failure strength and suggests that the material failed at higher loading. In the fracture surface of HDPE–GF–nanoclay–gMA system, the matrix surface shows the branched crack surface with several bright regions. This bright region is due to the extended deformation of the matrix before failure. The compatibilizing effect of gMA in nanoclay and matrix might have caused increased failure strain. In the case of HDPE–GF–microclay system, matrix fracture surface shows smooth crack surface. In gMA-filled and microclay-filled HDPE composites, the crack branching appears to be more than that of unfilled composites. This high crack branching may be resulted in improved strength and strain values in microclay and microclay–gMA-filled composites.

3.4. Wear characteristics

The wear properties of HDPE–clay and HDPE–clay–fiber series were examined and Table 8 shows the mass loss of composite series due to wear. Pure HDPE shows higher mass loss than the nanoclay-filled HDPE composites. The microclay-filled HDPE composites show marginal improvement in wear resistance. The gMA-filled HDPE–nanoclay composites show

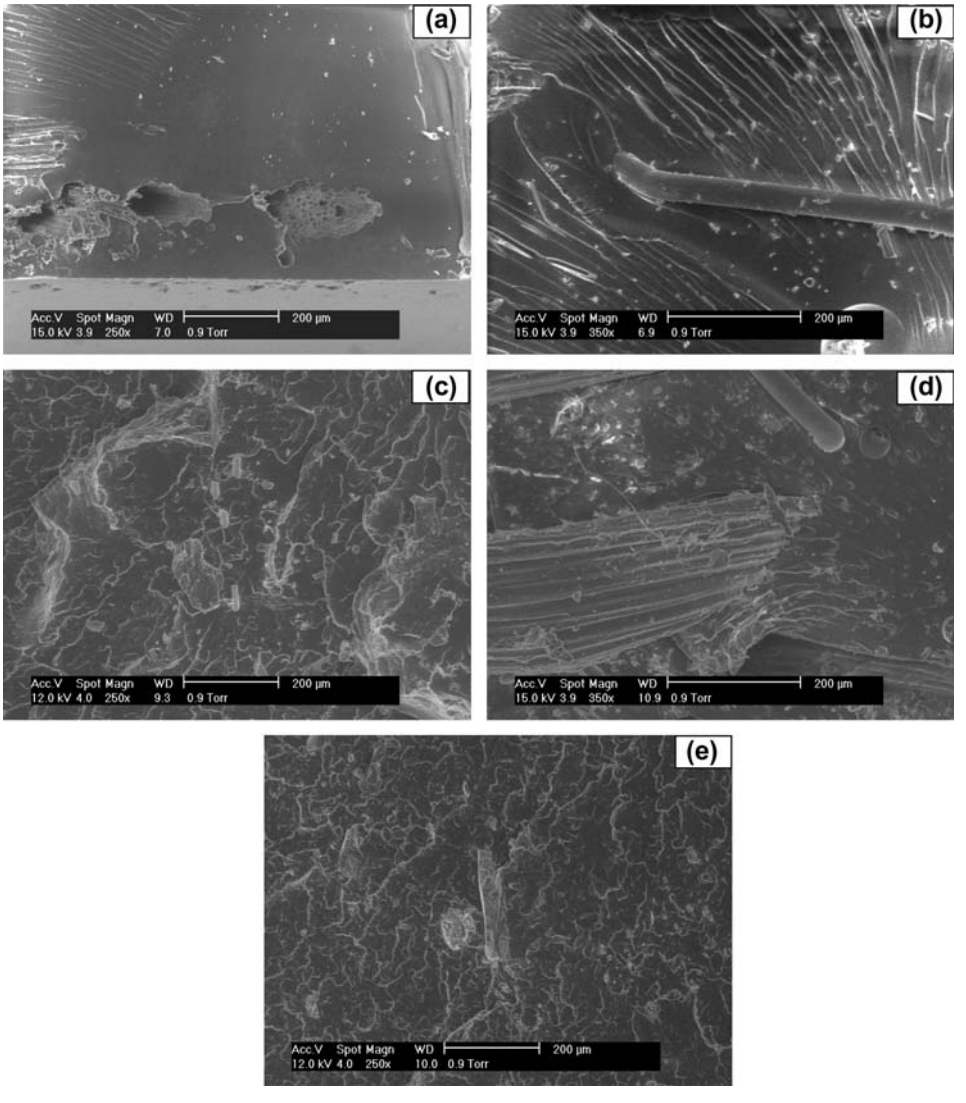

Figure 11. SEM pictures of tensile fracture surface of (a) HDPE + GF, (b) HDPE + GF + 3% nanoclay, (c) HDPE + GF + 3% nanoclay + 3% gMA, (d) HDPE + GF + 3% microclay, and (e) HDPE + GF + 3% microclay + 3% gMA.

improved wear resistance due to the good dispersions of particles in the matrix polymer. A similar trend of improved wear resistance was observed in GF-reinforced HDPE–nanoclay hybrid composites. If the particles agglomerate then the inter particle forces are weaker and during wear, these particles easily pull-out from the composites and thereby resulting in reduced wear property. Figure 12 shows the optical micrograph of wear surface of HDPE and HDPE–nanoclay–gMA specimen. In neat HDPE, the wear surface shows the presence of plowing marks. Similar wear loss of polypropylene-based nanocomposites due to plowing was observed elsewhere [31]. The mode of material removal was by the plowing action of the soft HDPE pin when subjected to the hard surface asperities of the brass counter disk. On

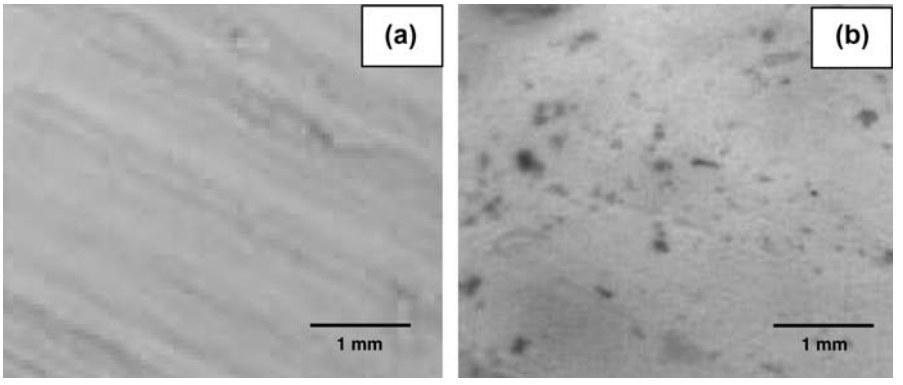

Figure 12. Optical microscope of wear surface of (a) HDPE and (b) HDPE–nanoclay–gMA.

the other hand, nanoclay-filled HDPE composite does not show such type of failure, suggesting that this material is harder than pure HDPE polymer. Nanoclay-filled HDPE makes material much harder to wear and thereby results in lower material loss.

4. Conclusions

A hybrid composite comprising HDPE polymer, nanoclay, and gMA compatibilizer was processed using the melt-blending technique. The effect of nanoclay addition on processing, structure, and properties of HDPE–GF composite was studied. In the first stage and second stage of this work, HDPE–clay composite and HDPE–GF–clay composites, respectively, were processed. Nanoclay addition increased the melt viscosity, crystalline fraction, and rate of crystallization of the HDPE polymer. Microclay addition did not affect crystallization property; however, it marginally increased the melt viscosity of HDPE polymer. It was observed that the distribution of clays in the polymer matrix was not good and shows agglomeration of particles in the matrix and therefore gMA compatibilizer was added. The addition of gMA in HDPE–clay system improved the dispersion of particles in polymer matrix and resulted in improved properties (tensile and wear) of composites. It also affected the melt viscosity and crystalline properties. Avarami equation suggests that the nanoclay acts as a nucleating agent and improves the crystallization behavior of HDPE polymer. The XRD and TEM results show the formation of exfoliated nanocomposite structure in nanoclay-filled HDPE polymer composites. Microclay addition, however, does not show the formation of nanolayer dispersion in HDPE polymer.

Acknowledgment

The authors gratefully acknowledges the financial support provided by National Research Foundation – NRF of South Africa (Grant No: 71599-2011) for carrying out this work.

References

[1] Jarukumjorn Kasama, Suppakarn Nitinat. Effect of glass fiber hybridization on properties of sisal fiber–polypropylene composites. Composites Part B. 2009;40:623–627.
[2] Zhuang Xingmin, Yan Xiong. Investigation of damage mechanisms in self-reinforced polyethylene composites by acoustic emission. Compos. Sci. Technol. 2006;66:444–449.
[3] Demir H, Atikler U, Balkose D, Tıhmınlıoglu F. The effect of fiber surface treatments on the tensile and water sorption properties of polypropylene–luffa fiber composites. Composites Part A. 2006;37:447–456.

[4] Seo Jung Min, Min Kyung Ho, Hwang Beong Bok, Lee In Chul, Ruchiranga Jayasekara Vishara, Jeon Han Yong, Jang Dong Hwan, Lim Joong Yeon. Experimental assessment of mechanical properties of geo-grid reinforced material and long-term performance of GT/HDPE, composite. Adv. Compos. Mater. 2008;17:247–258.
[5] Li Chaoqin, Zhang Yong, Zhang Yinxi, Zhang Changming. Rheological and mechanical properties of PC/HDPE/glass fiber composites. Polym. Polym. Compos. 2002;10:619–626.
[6] Tang Wenzhong, Santare Michael H, Advani Suresh G. Melt processing and mechanical property characterization of multi-walled carbon nanotube/high density polyethylene (MWNT/HDPE) composite films. Carbon. 2003;41:2779–2785.
[7] Varga CS, Miskolczi N, Bartha L, Lipoczi G. Improving the mechanical properties of glass-fibre-reinforced polyester composites by modification of fibre surface. Mater. Des. 2010;31:185–193.
[8] Angelo G Facca, Kortschot Mark T, Yan Ning. Predicting the tensile strength of natural fibre reinforced thermoplastics. Compos. Sci. Technol. 2007;67:2454–2466.
[9] Zou Yaobang, Yongcheng Feng Lu, Wang Xiaobo Liu. Processing and properties of MWNT/HDPE composites. Carbon. 2004;42:271–277.
[10] Li Yan, Chunjing Hu, Yehong Yu. Interfacial studies of sisal fiber reinforced high density polyethylene (HDPE) composites. Composites Part A. 2008;39:570–578.
[11] Mohanty Smita, Verma Sushil K, Nayak Sanjay K. Dynamic mechanical and thermal properties of MAPE treated jute/HDPE composites. Compos. Sci. Technol. 2006;66:538–547.
[12] Araujo R, Waldman WR, De Paoli MA. Thermal properties of high density polyethylene composites with natural fibres: coupling agent effect. Polym. Degrad. Stab. 2008;93:1770–1775.
[13] Tjong Sie Chin, Shi-Ai Xu, Li Robert Kwok-Yiu, Mai Yiu-Wing. Mechanical behavior and fracture toughness evaluation of maleic anhydride compatibilized short glass fiber/SEBS/polypropylene hybrid composites. Compos. Sci. Technol. 2002;62:831–840.
[14] Lotti Cybele, Isaac Claudia S, Branciforti Marcia C, Rosa MV, Susana Liberman Alves, Bretas Rosario ES. Rheological, mechanical and transport properties of blown films of high density polyethylene nanocomposites. Eur. Polym. J. 2008;44:1346–1357.
[15] Araujo EM, Barbosa R, Rodrigues AWB, Melo TJA, Ito EN. Processing and characterization of polyethylene/Brazilian clay nanocomposites. Mat. Sci. Eng: A. 2007;445–446:141–147.
[16] Maged A, Rupp Jorg EP, Suter Ulrich W. Tensile properties of polyethylene-layered silicate nanocomposites. Polymer. 2005;46:1653–1660.
[17] Minkova L, Peneva Y, Tashev E, Filippi S, Pracella M, Magagnini P. Thermal properties and microhardness of HDPE/clay nanocomposites compatibilized by different functionalized polyethylenes. Polym. Test. 2009;28:528–533.
[18] Zhao Chungui, Qin Huaili, Gong Fangling, Feng Meng, Zhang Shimin, Yang Mingshu. Mechanical, thermal and flammability properties of polyethylene/clay nanocomposites. Polym. Degrad. Stab. 2005;87:183–189.
[19] Lee Seung Hwan, Jae Ryoun Youn. Experimental and theoretical study on shear flow behavior of polypropylene/layered silicate nanocomposites. Adv. Compos. Mater. 2008;17:191–214.
[20] Spencer MW, Cui Lili, Yoo Youngjae, Paul DR. Morphology and properties of nanocomposites based on HDPE/HDPE-g-MA blends. Polymer. 2010;51:1056–1070.
[21] Mohaddespour A, Ahmadi SJ, Abolghasemi H, Jafarinejad SH. Investigation of mechanical, thermal and chemical properties of HDPE/PEG/OMT nanocomposites. J. Appl. Polym. Sci. 2007;7:2591–2597.
[22] Liang G, Xu J, Bao S, Xu W. Polyethylene/maleic anhydride grafted polyethylene/organic-montmorillonite nanocomposites, I. Preparation, microstructure, and mechanical properties. J. Appl. Polym. Sci. 2004;91:3974–3980.
[23] Faruk Omar, Matuana Laurent M. Nanoclay reinforced HDPE as a matrix for wood-plastic composites. Compos. Sci. Technol. 2008;68:2073–2077.
[24] Lin Li-Yu, Lee Joong-Hee, Hong Chang-Eui, Yoo Gye-Hyoung, Advani Suresh G. Preparation and characterization of layered silicate/glass fiber/epoxy hybrid nanocomposites via vacuum-assisted resin transfer molding (VARTM). Comp. Sci. Technol. 2006;66:2116–2125.
[25] Lei Yong, Qinglin Wu, Clemons Craig M, Yao Fei, Yanjun Xu. Influence of nanoclay on properties of HDPE/wood composites. J. Appl. Polym. Sci. 2007;106:3958–3966.
[26] Sarat K Swain, Isayev Avraam I. Effect of ultrasound on HDPE/clay nanocomposites: rheology structure and properties. Polymer. 2007;48:281–289.
[27] Tao Youji, Mai Kancheng. Non-isothermal crystallization and melting behavior of compatibilized polypropylene/recycled poly(ethylene terephthalate) blend. Eur. Polym. J. 2007;43:3538–3549.

[28] Chiu Fang-Chyou, Yen Hong-Zhi, Lee Cheng-En. Characterization of PP/HDPE blend based nanocomposites using different maleated polyolefins as compatibilizers. Polym. Test. 2010;29 (3):397–406.
[29] Dedecker K, Groeninckx G. Reactively compatibilized polymer blends: interfacial chemical reactions during melt-extrusion. Pure Appl. Chem. 1998;70:1289–1293.
[30] Viani A, Gualtieri A, Artioli G. The nature of disorder in montmorillonite by simulation of X-ray powder patterns. Am. Mineral. 2002;87:966–975.
[31] Kanny K, Jawahar P, Moodley VK. Mechanical and tribological behavior of clay-polypropylene nanocomposites. J. Mater. Sci. 2008;43:7230–7238.